Biochimica et Biophysica Acta 1807 (2011) 197–204

Contents lists available at ScienceDirect

Biochimica et Biophysica Acta

journal homepage: www.elsevier.com/locate/bbabio

How the N-terminal extremity of *Saccharomyces cerevisiae* IF1 interacts with ATP synthase: A kinetic approach

Tiona Andrianaivomananjaona [a,b], Martin Moune-Dimala [a,1], Sameh Herga [a], Violaine David [a], Francis Haraux [a,b,*]

[a] Service de Bioénergétique, Biologie Structurale et Mécanismes and CNRS-URA 2096, iBiTec-S, CEA Saclay, F 91191 Gif-sur-Yvette, France
[b] Univ Paris-Sud, LRA 17 V, F91405 Orsay, France

ARTICLE INFO

Article history:
Received 19 July 2010
Received in revised form 28 September 2010
Accepted 4 October 2010
Available online 14 October 2010

Keywords:
ATP synthase
IF1
Inhibitory peptide
Mitochondria
Yeast
Binding kinetics

ABSTRACT

The N-terminal part of the inhibitory peptide IF1 interacts with the central γ subunit of mitochondrial isolated extrinsic part of ATP synthase in the inhibited complex (J.R. Gledhill, M.G. Montgomery, G.W. Leslie, J.E. Walker, 2007). To explore its role in the different steps of IF1 binding, kinetics of inhibition of the isolated and membrane-bound enzymes were investigated using *Saccharomyces cerevisiae* IF1 derivatives modified in N-terminal extremity. First, we studied peptides truncated in Nter up to the amino acid immediately preceding Phe17, a well-conserved residue thought to play a key role. These deletions did not affect or even improve the access of IF1 to its target. They decreased the stability of the inhibited complex but much less than previously proposed. We also mutated IF1-Phe17 and found this amino acid not mandatory for the inhibitory effect. The most striking finding came from experiments in which PsaE, a 8 kDa globular-like protein, was attached in Nter of IF1. Unexpectedly, such a modification did not appreciably affect the rate of IF1 binding. Taken together, these data show that IF1-Nter plays no role in the recognition step but contributes to stabilize the inhibited complex. Moreover, the data obtained using chimeric PsaE-IF1 suggest that before binding IF1 presents to the enzyme with its middle part facing a catalytic interface and its Nter extremity folded in the opposite direction.

© 2010 Elsevier B.V. All rights reserved.

1. Introduction

ATP synthases (also called F_0F_1-ATPases) are anchored to bacterial cytoplasmic membranes, mitochondrial inner membranes, and chloroplast thylakoid membranes. These enzymatic complexes comprise an extrinsic F_1 domain ($\alpha_3\beta_3\gamma\delta\varepsilon$ in mitochondria) and a membranous F_0 domain connected by a central axis and a peripheral stalk. ATP synthases are rotary motors driven by the redox-generated protonmotive force (pmf) and they catalyze the condensation of ADP and inorganic phosphate into ATP [1]. Briefly, the pmf rotates a membranous oligomer of c subunits, the movement of which is transmitted to the central axis ($\gamma\delta\varepsilon$) that penetrates the catalytic domain $(\alpha\beta)_3$. This asymmetrical axis sequentially distorts the catalytic sites located at three $\alpha\beta$ interfaces, driving ATP synthesis. Its rotation has been directly observed in single molecule experiments [2], revealing the relationship between angular motion and catalytic steps [3,4].

Most ATP synthases preferentially work in the direction of ATP synthesis because they rapidly deactivate when the pmf collapses. In mitochondria, this process, which ensures specific inhibition of ATP hydrolysis but not of ATP synthesis, involves a soluble inhibitory peptide called IF1 [5]. IF1 binds to the catalytic domain of ATP synthase as soon as the latter starts to hydrolyze ATP, and it is released when the pmf is restored [6–14]. The reason for this differential binding/release is not yet understood; its elucidation requires to analyze the dynamics of IF1 binding. Previous studies have distinguished a first step, during which IF1 loosely binds to a catalytic site in an adequate conformation, and a second step, turnover-dependent, during which it is trapped within the complex [15,16].

IF1 is present in animals [5], yeasts [17,18], and plants [19,20]. It is a soluble peptide, 84 residues-long in *Bos taurus* and 63 residues-long in *Saccharomyces cerevisiae*. Its structure is essentially α-helical [21]. Pioneering investigations have shown that bovine IF1 (bIF1) lacking the first 16 residues after partial enzymatic digestion retains the capacity to inhibit ATPase activity [22]. It has been later reported that the minimal inhibitory sequence consists of residues 22–46 [23] or 14–47 [24] in bovine and of residues 17–41 in yeasts [23]. Deletion of the first 17 residues in mammal IF1 resulted in a still inhibitory peptide but with a very low affinity for ATP synthase, whereas conflicting results were

Abbreviations: F_0F_1-ATPase, ATP synthase complex (EC 3.6.3.14); F_1-ATPase, isolated extrinsic part of ATP synthase; IF1, endogenous inhibitory peptide of mitochondrial ATP synthase; bIF1, IF1 from bovine; yIF1, IF1 from yeast; SMP, submitochondrial particles; pmf, protonmotive force; SDS, sodium dodecyl sulfate; PVDF, polyvinylidene fluoride; Tris, tris(hydroxymethyl)aminomethane; MES, 2-(N-morpholino)ethanesulfonic acid; FCCP, carbonyl cyanide-p-trifluoromethoxyphenylhydrazone; Ni-NTA, nickel-nitrilotriacetic acid; TCA, trichloracetic acid

* Corresponding author. Service de Bioénergétique, Biologie Structurale et Mécanismes, bâtiment 532, CEA Saclay, F 91191 Gif-sur-Yvette, France. Fax: +33 1 69088717.
E-mail address: francis.haraux@cea.fr (F. Haraux).
[1] Present address: Institut de Génétique et de Biologie Moléculaire et Cellulaire, 1 rue Laurent Fries, 67404 Illkirch, France.

0005-2728/$ – see front matter © 2010 Elsevier B.V. All rights reserved.
doi:10.1016/j.bbabio.2010.10.002

reported concerning removal of the first 21 residues [23–25]. Binding parameters drawn from some of these early experiments [24,25] should be considered only qualitative because IF1 was pre-incubated with F_1-ATPase or submitochondrial particles (SMP) in a low pH buffer and ATP hydrolysis assayed after dilution into a high pH buffer. The X-ray structure of bovine F_1-ATPase in a complex with a truncated form of IF1 (residues 1–50) has been published [26]. In this structure, thought to be that of the dead-end, inhibited complex, IF1 interacts with α, β, and γ subunits. The C-terminal part of this inhibitory peptide (residues 22–50), which can be defined as the mid-part of the full peptide, is mainly associated with one of the three catalytic αβ interfaces, named $(\alpha\beta)_{DP}$ in reference to the structure of the non-inhibited complex. Importantly, the visible part in N-terminus of IF1 (residues 8–21) appears wrapped around the γ subunit and also interacting with the α_E subunit. This finding raises the problem of the role of the Nter part of IF1 in the different steps of the inhibitory process. IF1 peptides partially truncated in Nter have been shown to inhibit ATPase activity after several minutes of incubation [24,25], but *in vivo* the inhibitory peptide very rapidly responds to pmf variations, as shown by the absence of ATP hydrolysis activity immediately after adding an uncoupler to mitochondria [14]. Therefore, to understand the role of IF1 Nter extremity, it is necessary to study not only the affinity of IF1 derivatives for their target but also their kinetics of binding.

The aim of this work was to precise the role of the Nter extremity of yeast IF1 (yIF1) in the different steps of its binding to ATP synthase—approach, recognition, and locking. To reach this goal, we produced increasingly Nter-truncated yIF1 derivatives, up to the Phe17 residue, a well-conserved residue (Phe22 in bovine) thought to be critical for the inhibitory effect [27], and we investigated the consequences of these deletions on the kinetics of inhibition of ATP hydrolysis by yIF1, using isolated F_1-ATPase as well as SMP. Our data also lead to reconsider the importance for inhibition of the yIF1 Phe17 residue. Finally, whereas previous studies focused on partial deletions of IF1 Nter extremity, we also examined the consequences of attaching a small globular-like peptide to this part of the peptide. The effect of these yIF1 modifications on its kinetic constant of binding to the enzyme (k_{on}) and on the apparent dissociation constant of the complex at equilibrium (K_I) suggests an outline of the successive steps of IF1 binding.

2. Materials and methods

2.1. Molecular biology

DNA manipulations were carried out following published procedures [28] and the manufacturer recommendations unless otherwise indicated.

A series of variants of *inh1* gene deleted in the region encoding the yIF1 Nter extremity or mutated at a single position (yIF1 Δ1–13, Δ1–14, Δ1–15, Δ1–16, Δ1–,17 and F17S) was generated by PCR using pairs of primers shown in Table 1. PCR products were isolated after digestion by DpnI to eliminate matrix DNA. Plasmids were amplified in *Escherichia coli* (DH5RMCR strain) after transformation by electroporation using a Bio-Rad (Hercules, CA, USA) Gene Pulser electroporator.

PsaE gene encoding PsaE protein of *Synecchocystis sp. 6803* was subcloned from pRSET into pET30a$^+$ in 5′ extremity of *inh1*. *PsaE* and *inh1* were initially flanked by *NdeI* restriction site, respectively, in 3′ end and 5′ end. *Bam*H1 restriction site was added in pRSET (5′ end of *PsaE*) and pET30a$^+$ (upstream *NdeI*) by directed mutagenesis. *PsaE* was isolated from pRSET by digestion and cloned into pET30a$^+$ plasmid. Resulting plasmids were amplified in *E. coli* (DH5RMCR strain) after transformation by a thermal shock at 42 °C for 45 seconds. The full sequence of plasmids from kanamycin-resistant clones was checked (Eurofins MWG Operon, Ebersberg, Germany). DNA was purified using kits provided by Qiagen GmbH (Hilden, Germany) and by Macherey-Nagel EURL (Hoerdt, France).

2.2. Overexpression and purification of wT and mutated yIF1

pET30a$^+$ plasmids containing the wT or modified *inh1* gene were transformed into BL21(DE3) strain of *E.coli* by electroporation.

Selected clones were grown at 37 °C in liquid LB medium supplemented with 30 μg/mL kanamycin. After 2–3 hours, when the culture absorbance at 600 nm reached 0.6–0.8, yIF1 overexpression was triggered by adding 0.5 mM isopropyl-β-D-thiogalactopyranoside. After 3 hours, cells were harvested incubated for 1 hour at room temperature with 0.5 mg/mL lysozyme, 1 mM phenylmethylsulfonylfluoride (PMSF), 10 μg/mL RNase, and 10 μg/mL DNase and then briefly sonicated on ice. The lysate was centrifuged at 25,000 × *g* for 20 min (10 °C). The supernatant was incubated for 1 hour at room temperature, under gentle stirring, in a column containing Ni-NTA resin (3 mL, Qiagen GmbH, Hilden, Germany) prepared in buffer A (0.3 M NaCl and 50 mM Na_2HPO_4, pH 6.5) supplemented with 10 mM imidazole.

(i) Constructions of wT, truncated or mutated yIF1 had an enterokinase cleavage site between the His_6 N-terminal extension and the peptide of interest. Batches were washed with buffer A containing successively 10 and 20 mM imidazole. Then 2 mL of 20 mM Tris, 50 mM NaCl (pH 7.4) supplemented with 30 U of enterokinase was added on the column and the latter was incubated for 20 hours at room temperature under gentle shaking to cut the N-terminal extension. Protein of interest was eluted with 10 mM imidazole buffer A. Fractions containing proteins were pooled and heated at 90 °C for 10 min and centrifuged in a Benchtop Centrifuge to eliminate enterokinase. The supernatant was treated with 10% TCA at 4 °C for 5 min and centrifuged at 10 °C for 20 min. The pellet was solubilized with 50 mM Na-acetate, pH 5.5 and stored at −20 °C.

Table 1
Synthetic oligonucleotides used for mutagenesis of sequences encoding *Saccharomyces cerevisiae* IF1. The pET30a$^+$ plasmid contained *inh1* sequence with TTC encoding Phe28 replaced by TGG (Trp) to make protein purification easier. It was verified that this mutation does not change the functional properties of the produced protein and therefore this sequence is considered the wT. This plasmid was used for operations 2–4. The plasmid resulting from operation 4 (deletion Δ1–13) was used as starting plasmid for following deletions (operations 5–8). For operation 9, the starting pET30a$^+$ plasmid contained *inh1* sequence with either TTC (Phe) or TGG (Trp) encoding amino acid 28. yIF1 F17S and yIF1 F17S-F28W have identical functional properties.

Mutation	Oligonucleotides sequence (5′ to 3′)	Plasmid
1) Insertion of 9 codons spacer + *Bam*H1	GGTGATCAATTTAACGGTATAGGATGCGGATCCGGAGCCACCGCCGCTAGCAG	pRSET
2) Insertion of *Bam*H1	GGTACCGACGACGACGGATCCTCTGAAGGTTCTACCGGGC	pET30a$^+$
3) Addition His_6 in Nter PsaE-yIF1	GAAGGAGATATACAGATGCACCATCACCATCACCACGCCTTAAATCGTGG	pET30a$^+$
4) Deletion Δ1–13	CTGGGTACCGACGACGACGACAAGGAGGATTCGTTTGTTAAAAGGGAAAGG	pET30a$^+$
5) Deletion Δ1–14	CGACGACGACGACAAGGATTCGTTTGTTAAAAGGG	pET30a$^+$
6) Deletion Δ1–15	CGACGACGACGACAAGTCGTTTGTTAAAAGGG	pET30a$^+$
7) Deletion Δ1–16	CGACGACGACGACAAGTTTGTTAAAAGGGAAAG	pET30a$^+$
8) Deletion Δ1–17	CGACGACGACGACAAGGTTAAAAGGGAAAGGG	pET30a$^+$
9) Mutation F17S	GTCAAGCTCAGAGGATTCGTCTGTTAAAAGGGAAAG	pET30a$^+$

(ii) After washing with 10 mM imidazole and 20 mM imidazole buffer A, His-tagged PsaE-yIF1 protein was eluted with 250 mM imidazole buffer A. The pooled fractions were dialyzed for 7 hours at room temperature against 50 mM NaCl, 20 Mm Tris, pH 7.8. Protein was concentrated using Ultrafree®-0.5 Centrifugal Filter Device (cutoff = 5000) (Millipore, Bedford, MA, USA) and stored.

Protein concentration was determined using micro-BCA titration kit (Pierce Chemical Co., Rockford, IL, USA).

2.3. Characterization of peptides

Purified peptides were analyzed by SDS–PAGE (12%) and revealed with Coomassie blue R250.

For immunoblotting, proteins were electrotransferred onto Hybond-P PVDF membrane (Amersham, Little Chalfont, UK) previously activated with methanol. The membrane was then saturated for 1 hour at room temperature with 5% milk in Na-phosphate 10 mM, NaCl 150 mM, 0.5% Tween 20, pH 7.4 (TPBS). Rabbit polyclonal antibodies specific to IF1 or mouse polyclonal antibodies specific to PsaE in 0.5% milk TPBS were applied overnight at 4 °C. After extensive washes, goat anti-rabbit antibodies or goat anti-mouse antibodies coupled to alkaline phosphatase were applied for 1 hour at room temperature. Phosphatase activity was revealed by colorimetry using BCIP–NBT.

Theoretical electrical charge of the peptides at pH 6.5 was calculated from the formula: $q = \Sigma[n_i/(1+10^{6.5-\mathrm{pK}i})] - \Sigma[n_j/(1+10^{\mathrm{pk}j-6.5})]$, where i refers to basic residues (Nter, Arg, Lys, His) and j refers to acidic residues (Asp, Glu, Cys, Tyr, Cter). The calculated values (number of positive elementary charges per molecule) are +2.3 (yIF1 wT, yIF1 Δ1–13, yIF1 F17S), +3.3 (yIF1 Δ1–14), +4.3 (yIF1 Δ1–15, yIF1 Δ1–16), and +4.9 (PsaE-yIF1).

2.4. Preparation of submitochondrial particles (SMP) and purified F_1-ATPase

S. cerevisiae cells (Euroscarf BY4741 *MAT a, his3Δ1, leu2Δ0, met15Δ0, ura3Δ0*) were grown at 28 °C in a large volume of strictly respiratory medium containing 1% yeast extract, 0.1% KH_2PO_4, 0.12% $SO_4(NH_4)_2$, 2% lactate, 60 mg/L leucine, 60 mg/L histidine, 20 mg/L uracile, 40 mg/L methionine, pH 5.5. yIF1-stripped SMP and F_1-ATPase were prepared from cells harvested in exponential phase as previously described [14,16].

2.5. ATP hydrolysis measurement and kinetic analysis

Continuous monitoring of ATP hydrolysis by F_1-ATPase or SMP coupled to NADH oxidation was carried out spectrophotometrically as described [14]. The reaction was observed in a stirred and thermostated cuvette (25 °C) containing 50 mM MES pH 6.5, 20 mM KCl, 1 mM $MgCl_2$, 1 mM phosphoenolpyruvate, 20 U/mL pyruvate kinase, 50 U/mL lactate dehydrogenase, 0.4 mM NADH, and 1 mM MgATP. In the case of SMP, the buffer also contained 1.5 μM antimycin and 1.5 μM FCCP. ATP hydrolysis was initiated by adding F_1-ATPase or SMP and monitored by NADH absorbance decrease at 340 nm. After 2–4 min, yIF1 wT or modified peptide was injected and ATPase activity decayed. The spectrophotometric recording was fitted to the following function corresponding to a monoexponential decay of the ATPase activity:

$$y(t) = V(\mathrm{I})\mathrm{t} + \left[(V(0)-V(\mathrm{I}))/k_{\mathrm{app}}\right]\left[1-\exp\left(-k_{\mathrm{app}}t\right)\right] + y_0 \qquad (1)$$

where $y(t)$ is the absorbance at time t, and y_0 the absorbance at zero time defined as the time of IF1 addition. $V(0)$ is the constant rate of absorbance variation before IF1 addition in absorbance units per second (proportional to the initial ATPase activity), $V(\mathrm{I})$ the final rate of absorbance variation after IF1 addition (proportional to the final ATPase activity), and k_{app} the apparent inhibition rate constant in s^{-1}. The obtained k_{app} value was plotted as a function of the inhibitor concentration $[I]$ to determine the rate constants k_{on} (in $M^{-1}\ s^{-1}$) and k_{off} (in s^{-1}) according to:

$$k_{\mathrm{app}} = k_{\mathrm{on}}[I] + k_{\mathrm{off}} \qquad (2)$$

The relation between the $V(\mathrm{I})/V(0)$ ratio and the inhibitor concentration was fitted to the following function:

$$V(\mathrm{I})/V(0) = v_{\mathrm{r}} + (1-v_{\mathrm{r}})/(1 + [I]/K_{\mathrm{I}}) \qquad (3)$$

where v_{r} is the inhibitor-insensitive fraction of $V(0)$ (always lower than 5%). Theoretically, K_{I} should be equal to the $k_{\mathrm{off}}/k_{\mathrm{on}}$ ratio. In all of the experiments, the inhibitor concentration was much higher than the enzyme concentration. Therefore, the total and free concentrations of inhibitor could be considered identical and constant during the kinetics of inhibition. This justifies the monoexponential analysis of the decay (Eq. (1)) and the hyperbolic analysis of the inhibition at equilibrium (Eq. (3)).

It has been shown [15,16] that the measured rate binding constant k_{on} of IF1 depends on MgATP concentration because it is actually modulated by the nucleotide occupancy and the catalytic turnover of F_1-ATPase. Experiments reported here were carried out with 1 mM MgATP. At this MgATP concentration, the k_{on} value reaches a plateau and represents the true rate binding constant [15,16].

2.6. Chemicals and reagents

All reagents were of analytical grade. PCR mutagenesis was carried out using the QuikChange Site-Directed Mutagenesis Kit from Stratagene (La Jolla, CA, USA). DNA ligase was from New England Biolabs (Ipswitch, MA, USA). BCIP (5-bromo-4-chloro-3-indolyl phosphate) and NBT (nitro blue tetrazolium) were from Bethesda Research Laboratories (Gaithersburg, MD, USA). The yeast extract was from Difco (Detroit, MI, USA). ATP, NADH, phosphoenolpyruvate, pyruvate kinase, and lactate dehydrogenase were purchased from Roche (Basel, Switzerland).

pRSET plasmid containing the *PsaE* gene, PsaE protein, and anti-PsaE antibody were kindly provided by Dr Bernard Lagoutte (SB^2SM, CEA Saclay). Anti-IF1 antibody was a generous gift of Dr Kunio Tagawa (Osaka, Japan).

3. Results

3.1. Obtaining purified yIF1-derived peptides

Fig. 1a shows the position of IF1 in the crystallized bovine F_1-IF1 complex [26], the structure of which will be the reference throughout this study. Visible IF1 amino acids close to the F_1-ATPase γ subunit (residues 8–21) are represented in ball-and-sticks. bIF1 Phe22 (analog to yIF1 Phe17), in full atoms, marks the beginning of the highly conserved IF1 sequence part (Fig. 1c) drawn as α-helix. Fig. 1c represents the yIF1 truncated forms that were obtained, with 13, 14, 15, and 16 residues removed. The maximal deletion, Δ1–16, stops just before the conserved Phe17. We have also produced a chimeric peptide in which PsaE, a component of Photosystem I (here from the cyanobacterium *Synechocystis sp.* PCC 6803) was attached to the Nter extremity of yIF1 *via* a 9 residues spacer. This peptide (PsaE-yIF1) was His-tagged in Nter. Cyanobacterial PsaE [29] and bovine F_1-ATPase in complex with bIF1 [26] are represented at the same scale in Fig. 1b. Fig. 2 shows SDS–PAGE analysis of wT and truncated forms of yIF1 (a) and of wT yIF1, PsaE, and PsaE-yIF1 (b). No significant contaminant

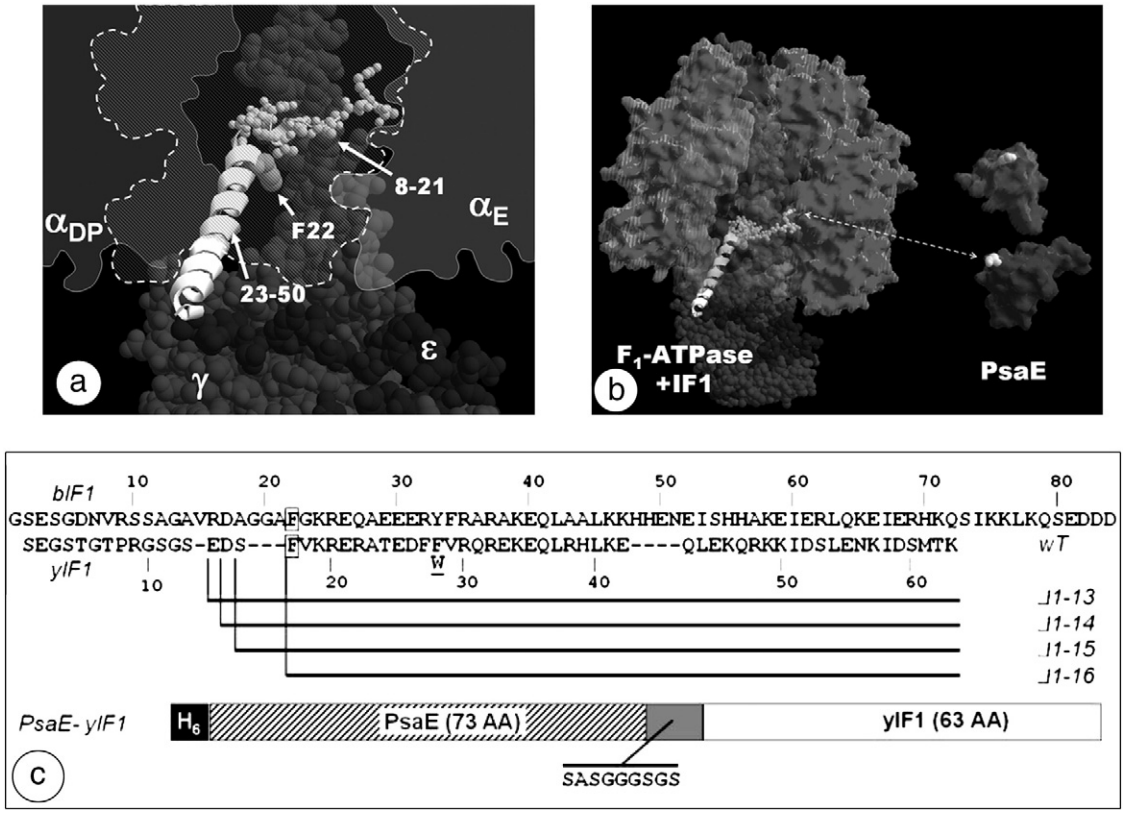

Fig. 1. Position of bovine IF1 in the inhibited complex and sequence of modified yeast IF1 peptides prepared for this study. Panel a, mitochondrial F_1-ATPase in complex with IF1 truncated in the C-terminal (reference 26, pdb entry *2v7q*; image edited using Swiss-pdbViewer software). Subunits α_{DP} (left), β_{DP} (middle, forefront), and α_E (right) are represented by transparent shapes. Phe22 (full atoms) is a highly conserved amino acid. The helical region of IF1 from Phe22 to Glu50 is trapped between α_{DP} and β_{DP}. IF1 residues from Val8 to Ala21 (ball-and-sticks) form a hook-shaped structure around the central axis of F_1 formed by the γ subunit. Panel b, image showing the respective sizes of inhibited F_1-ATPase complex and PsaE protein (pdb entry *1gxi*). PsaE is represented under two different orientations and its C-terminal residue is highlighted. In PsaE-yIF1 chimera, this residue was linked to the Nter extremity of yIF1. Panel c, sequence alignment of *Bos taurus* IF1 (bIF1) and *Saccharomyces cerevisiae* IF1 (yIF1) and definition of the different yIF1-derived peptides prepared for this study. The conserved Phe22 (bovine) or Phe17 (yeast) is boxed. Unless otherwise stated, Phe28 (yeast numbering) was replaced by Trp (underlined) to facilitate the peptide detection during purification. Δ1–13, Δ1–14, Δ1–15, Δ1–16, peptides truncated in Nter. Sequence of PsaE-yIF1 chimera symbolized by a bar; from left to right, hexahistidine tag in Nter (black), PsaE (hatched), nine residues spacer (gray), and yIF1 (white).

was detected. In Fig. 2c, immunoblots of wT yIF1, PsaE, and PsaE-yIF1 realized using anti-IF1 and anti-PsaE antibodies are displayed. As expected, PsaE-IF1 was detected as a single band using each antibody.

3.2. Kinetics of inhibition of ATP hydrolysis by yIF1 truncated forms

All of the experiments were carried out at pH 6.5, which is lower than matricial pH *in vivo*. This pH value was chosen to allow better comparisons with previous reports. Moreover, at higher pH, it may become very difficult, for some derivatives, to estimate at the same time the rate and the extent of inhibition. From previous work, at higher pH, k_{on} is expected to decrease and k_{off} expected to decrease [14]. Other differences with *in vivo* situation are the very low concentrations of enzyme and a large excess of yIF1, which remains however well below its putative matricial concentration. These conditions are required for kinetic studies. Fig. 3 shows typical kinetics of F_1-ATPase inhibition by wT yIF1 (a) and by its truncated derivative lacking the first 15 residues (b). Both peptides were added at increasing concentrations. For yIF1 wT (a), the final inhibition is almost completely independent of the inhibitor concentration. This indicates that the lowest inhibitor concentration used here was much higher than the K_I (or K_d) value. The rate of inhibition increases with IF1 concentration, which indicates that it is controlled by the rate of IF1 binding. With the Δ1–15 derivative (b), not only the rate of

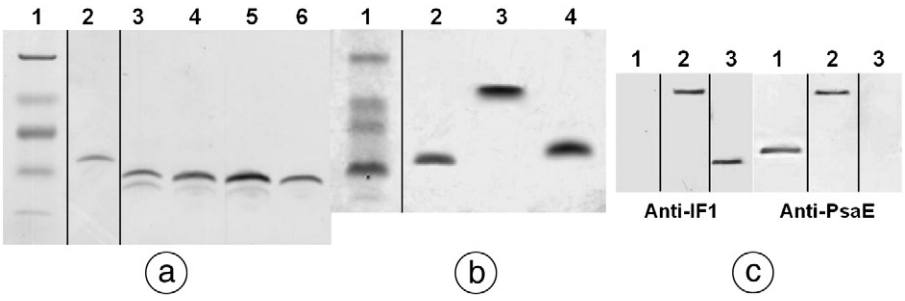

Fig. 2. Analysis of purified recombinant yeast IF1 and derivatives. Conditions as described under Materials and methods. One microgram of each peptide was loaded and analyzed by SDS–PAGE. Panels a and b, Coomassie blue staining. Panel c, immunoblotting using antibodies specific to yIF1 (left) or PsaE (right). Panel a, lanes: (1) marker proteins, molecular weights 26.6, 17, 14.2, 6.5, and 3.5 kDa, (2) wT yIF1, (3) yIF1 Δ1–13, (4) yIF1 Δ1–14, (5) yIF1 Δ1–15, and (6) yIF1 Δ1–16. Panel b, lanes: (1) marker proteins, (2) wT yIF1, (3) PsaE-yIF1, and (4) PsaE. Panel c, lanes: (1) PsaE, (2) PsaE-yIF1, and (3) wT yIF1.

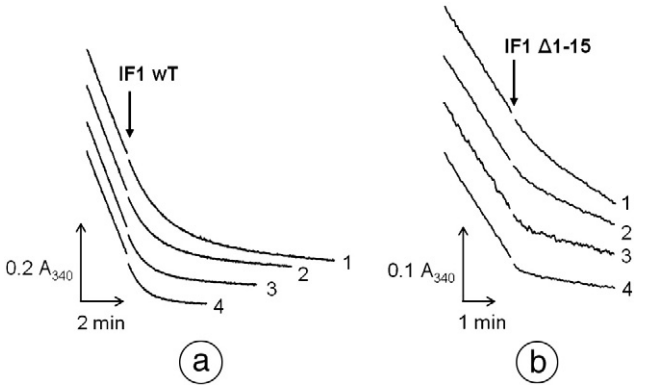

Fig. 3. Time course of ATP hydrolysis and ATPase inhibition monitored by NADH absorbance at 340 nm. Conditions as described under Materials and methods. Inhibitor additions indicated by vertical arrows. Panel a, additions of yIF1 wT 30 nM (curve 1), 50 nM (curve 2), 70 nM (curve 3), 100 nM (curve 4) to 1.5 nM F_1-ATPase. Panel b, additions of yIF1 Δ1–15 10 nM (curve 1), 20 nM (curve 2), 50 nM (curve 3), 100 nM (curve 4) to 0.8 nM F_1-ATPase.

Table 2
Binding parameters of yIF1 and derivatives determined on isolated F_1-ATPase (without brackets) and on submitochondrial particles (under brackets). Values calculated from the data used to build Fig. 4 (isolated F_1-ATPase) or from similar data (SMP). Fitting was performed on non-averaged data to better estimate uncertainties of the parameters. Indicated uncertainties are those provided by the software (Microcal Origin®). k_{on} was given by the slope value in the linear Eq. (2) (Materials and methods). The constant K_I (theoretically identical to the equilibrium dissociation constant K_d) was given by the hyperbolic Eq. (3). k_{off} was given by the $K_I k_{on}$ product. Theoretically, k_{off} could also be given by the intercept, but this value is less precise (see Supplementary material) The k_{on} value of yIF1 F17S, and therefore the k_{off} value, are approximate (see text).

Peptide	k_{on} (M^{-1} s^{-1})	K_I (nM)	k_{off} (s^{-1})
yIF1 wT	$3.2 \pm 0.3 \times 10^5$	<1	nd
	[$2.2 \pm 0.2 \times 10^5$]	[<1]	[nd]
yIF1 Δ1–13	$3.9 \pm 0.2 \times 10^5$	<1	nd
	[$2.7 \pm 0.3 \times 10^5$]	[<1]	[nd]
yIF1 Δ1–14	$3.3 \pm 0.3 \times 10^5$	2.9 ± 0.5	$9.6 \pm 2.5 \times 10^{-4}$
	[$8.1 \pm 0.5 \times 10^5$]	[<1]	[nd]
yIF1 Δ1–15	$6.5 \pm 0.9 \times 10^5$	4.4 ± 0.7	$2.9 \pm 0.9 \times 10^{-3}$
	[$17.0 \pm 1.0 \times 10^5$]	[1.8 ± 0.2]	[$3.1 \pm 0.5 \times 10^{-3}$]
yIF1 Δ1–16	$9.1 \pm 1.8 \times 10^5$	20.3 ± 2.1	$1.9 \pm 0.6 \times 10^{-2}$
	[$19.2 \pm 1.9 \times 10^5$]	[8.1 ± 1.9]	[$1.6 \pm 0.5 \times 10^{-2}$]
PsaE-yIF1	$2.6 \pm 0.1 \times 10^5$	10.9 ± 1.5	$2.8 \pm 0.5 \times 10^{-3}$
	[$1.7 \pm 0.1 \times 10^5$]	[6.4 ± 0.8]	[$1.1 \pm 0.2 \times 10^{-3}$]
yIF1 F17S	$7.2 \pm 1.4 \times 10^5$	56.2 ± 3.7	$4.1 \pm 1.1 \times 10^{-2}$
	[$2.4 \pm 0.5 \times 10^5$]	[185 ± 14]	[$4.4 \pm 1.3 \times 10^{-2}$]

inhibition but also the final degree of inhibition increases with peptide concentration. This means that its K_d value is not negligible with respect to the inhibitor concentrations used.

All the progression curves like those displayed in Fig. 3 could be satisfactorily fitted using a kinetic model in which the instantaneous rate of ATP hydrolysis after inhibitor addition exponentially decays with time, from its initial value $V(0)$ to a final value $V(I)$ [15,30] (see also Eq. (1)). The time constant of the exponential decay (k_{app}) is the apparent constant of inhibition. k_{app} was previously shown to be a linear function of IF1 concentration, the proportionality coefficient of which gives the value of the rate constant of binding of IF1 to the enzyme [14,30]. This linear relationship remains valid for all the truncated forms of yIF1 (Fig. 4a). It is practically the same for yIF1 wT (closed circles), yIF1 Δ1–13 (closed triangles), and yIF1 Δ1–14 (open triangles). Therefore, removing the first 13 or 14 residues does not significantly affect the k_{on} value as given by the slope of the plot (3.2×10^5 M^{-1} s^{-1} for wT). On the other hand, removing the first 15 or 16 residues increases the k_{on} value (about 9×10^5 M^{-1} s^{-1} for Δ1–16).

The extent of inhibition at the end of the inhibition kinetics was given by the expression $1 - V(I)/V(0)$. It was plotted as a function of yIF1 derivatives concentration (Fig. 4b). At the lowest concentration used (20 nM), yIF1 wT inhibits ATP hydrolysis by practically 100%, showing that the K_I value is well below this concentration, as previously observed [14]. The pattern is almost the same for yIF1 Δ1–13. Deletion of the first 14, 15, and 16 residues progressively decreases the affinity of the inhibitory peptide for F_1-ATPase, as shown by the higher inhibitor concentrations required to obtain a given level of inhibition. In all cases, F_1-ATPase activity is almost fully inhibited at saturating concentration of IF1 derivative.

The results are summarized in Table 2, in which the k_{off} values have been calculated from the product K_I k_{on}. k_{off} cannot be estimated for yIF1 wT, but it can hardly exceed 10^{-4} s^{-1}. Removal of Nter residues results in a dramatic increase of k_{off} (more than 100-fold), much more important than k_{on} increase (3-fold) when the first 16th residues have been removed. So the interaction of the Nter extremity of yIF1 is important for the stabilization of the inhibited complex. Experiments were also carried out using submitochondrial particles instead of purified F_1-ATPase (Table 2, data under brackets). The k_{on} value of yIF1 wT is decreased by about 30%. This moderate decrease reflects a more difficult access of IF1 to its binding site in SMP, probably due to the

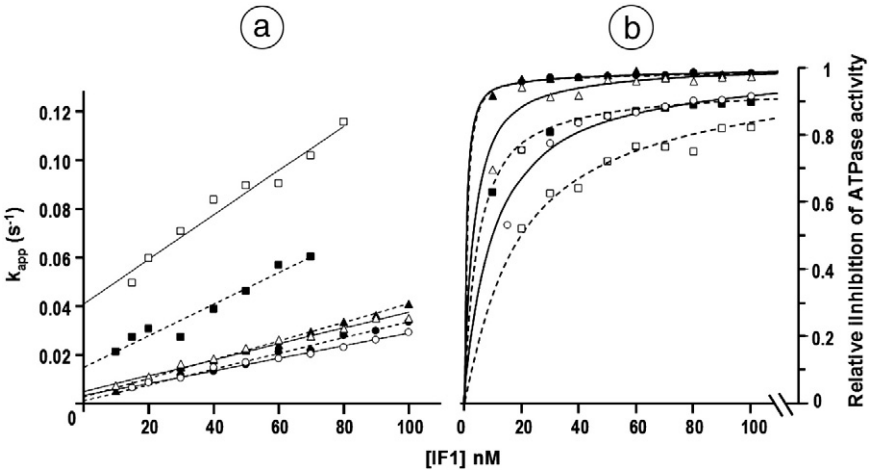

Fig. 4. Rate constant of inhibition (k_{app}) (a) and maximal extent of inhibition (b) of isolated F_1-ATPase as a function of yIF1 derivatives concentration. Conditions as in Fig. 3. (—●—) yIF1 wT; (--▲--) yIF1 Δ1–13; (—Δ—) yIF1 Δ1–14; (--■--) yIF1 Δ1–15; (—□—) yIF1 Δ1–16; (—○—) PsaE-yIF1. Each data point represents the average of six independent estimates for yIF1 wT and three independent estimates for derivatives. Kinetic analysis performed as described under Materials and methods, Eq. (1). Continuous lines were obtained by fitting each data set with a linear regression (Materials and methods, Eq. (2)) or with a hyperbolic model of inhibition (Materials and methods, Eq. (3)).

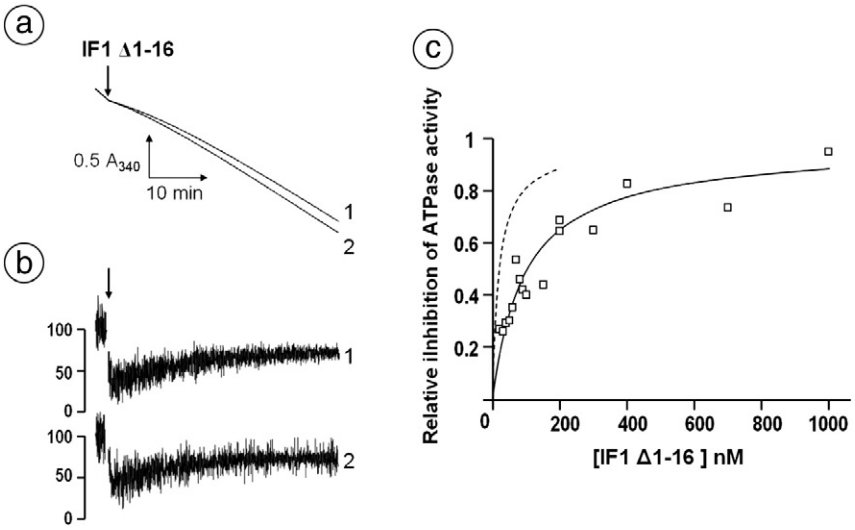

Fig. 5. Partial reactivation of F_1-ATPase activity after inhibition by yIF1 Δ1–16. Conditions as in Fig. 3 except for the time range. Panel a, time course of ATP hydrolysis showing the fast inhibition following yIF1 Δ1–16 addition (vertical arrow) and the subsequent slow reactivation. Curve 1, 40 nM yIF1 Δ1–16; curve 2, 20 nM yIF1 Δ1–16. Panel b, instantaneous rate of ATP hydrolysis versus time obtained from the first derivative of the two spectrophotometer recordings displayed in panel a (same time scale). Rates expressed as percentage of the rate before inhibitor addition. Panel c, remaining extent of inhibition at the end of the reactivation phase as a function of inhibitor concentration. The dashed curve recalls the extent of inhibition obtained before the reactivation phase (see Fig. 4b).

presence of the peripheral stalk of ATP synthase and maybe also to the supramolecular organization of the complexes [31]. As in the case of isolated F_1-ATPase, deletion of Nter residues results in k_{on} increase. Remarkably, the k_{on} values for yIF1 Δ1–14, Δ1–15, and Δ1–16 are even higher than when using isolated F_1-ATPase subcomplex. This suggests that a non-steric factor is involved here (see Discussion).

F_1-ATPase inhibited by yIF1 wT, Δ1–13, and Δ1–14 remained permanently inactive. After yIF1 Δ1–15 or Δ1–16 addition, ATPase activity first reached a minimum corresponding to the levels of inhibition plotted in Fig. 4b and then slowly increased. This reactivation was most pronounced in the case of yIF1 Δ1–16. Fig. 5a shows the time course of F_1-ATPase inhibition and reactivation over a long time range, at two concentrations of yIF1 Δ1–16. The final recovery of activity is only partial (Fig. 5b). The remaining extent of ATPase inhibition at the end of the reactivation decreases with yIF1 Δ1–16 concentration (Fig. 5c). As compared to the transient inhibition reported in Fig. 4b (see also Fig. 5c, dashed curve), the concentrations of yIF1 Δ1–16 required to obtain the same inhibition is about 5 times higher.Since Phe17 is highly conserved and was reported to play a key role [27], we also prepared the Δ1–17 truncated form. We found that this peptide might be able to inhibit the F_1-ATPase (results not shown). Unfortunately, it proved to be difficult to purify, to be very unstable and sensitive to degradation. As a consequence, no clear conclusion could be drawn about its inhibitory properties.

3.3. Effect of F17S mutation on yIF1 inhibitory properties

The role of Phe17 was investigated using yIF1 F17S, which was previously reported to bind to ATP synthase in a non-inhibitory way [27]. Unexpectedly, we found that yIF1 F17S was able to fully inhibit F_1-ATPase but with a much lower affinity than yIF1 wT and even than the Nter-truncated derivatives: the K_I value is about 60 nM with isolated F_1-ATPase and about 180 nM with SMP (Table 2; see also Supplementary material). When this peptide was submitted to trypsin proteolysis, its inhibitory power fully disappeared (data not shown), which rules out any unspecific effect.

As for the truncated peptides, we also estimated the k_{on} value of yIF1 F17S. This was especially difficult because the inhibition was very fast and therefore its kinetics could be only resolved in a low inhibitor concentration range, where the final inhibition was not complete. However, using F_1-ATPase, k_{on} could be grossly estimated to $7\times10^5\ M^{-1}\ s^{-1}$, 2.5-fold the measured value for yIF1 wT, and using SMP, estimated to $2\times10^5\ M^{-1}\ s^{-1}$, about the same value for yIF1 wT (Table 2). So the F17S mutation acts on k_{off}, not on k_{on}.

3.4. Inhibition of ATP hydrolysis by PsaE-yIF1, a chimeric protein

In the bovine IF1-inhibited complex, IF1 deeply penetrates the F_1-ATPase and interacts with its central γ subunit by its Nter extremity [26]. Attaching a bulky object to this extremity is therefore expected to dramatically affect IF1 binding to the enzyme. To check this hypothesis we produced a chimeric peptide in which the Nter extremity of wT yIF1 was connected to PsaE, a globular-like protein, *via* a short spacer (Figs. 1b and c). The 3D structure of PsaE is known, and this protein has a sufficient size to notably increase the steric hindrance at Nter extremity of yIF1. Unexpectedly, the chimeric PsaE-yIF1 peptide proved to fully inhibit ATPase activity with almost the same binding rate constant for yIF1 wT (Fig. 4a, Table 2). It was verified that PsaE protein alone had no effect on ATP hydrolysis (control not shown). The k_{on} values of PsaE-yIF1 are about $2.6\times10^5\ M^{-1}\ s^{-1}$ with isolated F_1-ATPase and $1.7\times10^5\ M^{-1}\ s^{-1}$ with SMP, that is 80% of the values determined for yIF1 wT (Table 2). Thus, a considerable increase of steric hindrance in Nter (Fig. 1b) has a very limited effect on the recognition of IF1 binding site. The stability of the inhibited complex is more sensitive to this modification, as shown by the significant increase of K_I and k_{off}.

4. Discussion

4.1. Modifications of yIF1 inhibitory properties induced by progressive truncation of its Nter extremity

The structure of bovine F_1-ATPase in complex with IF1 shows that the Nter extremity of the inhibitory peptide interacts with the central part of the enzyme [26]. This suggests that its entry into the enzyme is the first step of binding. For the first time, it was possible here to observe the effect of modifications of the inhibitory peptide IF1 both on its kinetic binding constant (k_{on}) and on the dissociation constant of the inhibited complex (estimated by K_I), indirectly estimated from the concentration dependency of the rate and extent of inhibition. Using purified F_1-ATPase, removing the first 14 residues of yIF1 does not change k_{on} and somewhat increases K_I (Table 2). This indicates

that these residues play no role in approach and recognition of yIF1 binding site. Deleting further the two next residues increases k_{on} and K_I. This suggests that residues 15 and 16 somewhat hamper the early step of binding. However, they are needed in the next step because they contribute, as residue 14, to the stabilization of the inhibited complex. Whereas k_{on} is increased by a factor 3 by the removal of residues 15 and 16, k_{off} indeed is increased by a factor 20.

With yIF1 Δ1–15 and yIF1 Δ1–16, the inhibited complex slowly reactivates (Fig. 5). Such a reactivation has been previously observed in some Nter truncated mutants [24]. However, in those experiments, the sample pre-incubated with the inhibitor at low pH was checked for ATP hydrolysis after a dilution step, which favors IF1 release. Here, reactivation is not due to dilution but probably due to a slow conversion of the inhibited F_1-ATPase into a form with a low affinity for IF1 and/or to some instability of the peptide. Whatever it may be, this reactivation phenomenon may make K_I determination ambiguous. In the case of yIF1 Δ1–16, in which reactivation is most pronounced, two different K_I values are actually determined, one before ($K_I = 20$ nM) and one after ($K_I = 100$ nM, Fig. 6c) reactivation. Even the latter value remains well below all previously reported K_I values of inhibitory peptides similarly truncated in Nter [23].

In the crystallized bovine F_1-ATPase in complex with IF1, the two residues immediately preceding the conserved Phe21 (Phe17 in yeast) do not interact with the central γ subunit. This suggests that stabilization of the yeast inhibited complex by residues 15–16 does not involve γ subunit, but the fact that these residues are not conserved and that the structure of the yeast inhibited complex is not yet available forbids definite conclusion.

As expected from the slightly diminished accessibility of IF1 binding site in SMP, yIF1 wT and yIF1 Δ1–13 bind a little bit more slowly to the membrane-bound ATP synthase than to the isolated F_1-ATPase subcomplex. The different yIF1 modifications have qualitatively the same consequences with the membrane-bound enzyme as with the solubilized one, except that k_{on} increase starts from the removal of the 14th (instead of the 13th) residue and is more pronounced after removing residues 15 and 16. Contrary to yIF1 wT and yIF1 Δ1–13, yIF1 Δ1–14, yIF1 Δ1–15, and yIF1 Δ1–16 bind more rapidly to membrane-bound ATP synthase than to isolated F_1-ATPase. A possible explanation is the fact that, at pH 6.5, yIF1 and derivatives are positively charged and are therefore expected to somewhat accumulate near the membrane that is negatively charged [32]. In the case of yIF1 wT and yIF1 Δ1–13, the net charge (theoretically 2.3 positive charges per molecule) is not high enough to balance the steric effects of the membranous environment and k_{on} is globally decreased in SMP. With the significant charge increase of yIF1 Δ1–14 (3.3 charges), Δ1–15 (4.3 charges), and Δ1–16 (4.3 charges) due to loss of acidic residues, the electrostatic effect can outmatch the steric effect. Interestingly, the k_{off} value, which is not expected to depend on the local yIF1 concentration, is the same with SMP and isolated F_1-ATPase in the case of yIF1 Δ1–15 and yIF1 Δ1–16.

4.2. Re-examined importance of the conserved phenylalanine 17

The amino acid immediately following residues 15–16 (Phe17) is a kind of milestone in IF1 sequence. It is the starting point of the well-conserved inhibitory sequence. In crystallized inhibited bovine F_1-ATPase, its counterpart Phe22 marks the border between the Nter part of IF1 wrapped around the γ subunit and its mid-part locked between α_{DP} and β_{DP}. Mutation of Phe17 into serine was previously reported to make the peptide non-inhibitory at concentrations up to 5 μM. Moreover, yIF1 F17S was proposed to competitively prevent inhibition by yIF1 wT [27]. In the present work, yIF1 F17S proved to inhibit isolated F_1-ATPase as well as membrane-bound F_0F_1-ATPase with a K_I value of 60 and 180 nM, respectively (Table 2). This discrepancy can be at least partially explained by the fact that previous investigators measured ATPase activity of the yIF1-pretreated sample after diluting it 50-fold in a high pH medium. In particular, the apparently silent binding of yIF1 F17S could be due to a true competition during the incubation stage, followed by a release of yIF1 F17S without yIF1 wT binding after the dilution. To conclude, Phe17 is not mandatory for the inhibitory effect and silent binding of yIF1 F17S is unlikely. However, Phe17 contributes to the stability of the inhibited complex. This is not unexpected since in the crystallized bovine inhibited complex, Phe22 is mainly surrounded by the conserved hydrophobic residues β_{DP}A389, β_{TP}I390, β_{TP}L391, and γI16.

4.3. Reappraisal of previous results

The effect of significant Nter deletions of mammal [22–25] and yeast [23] IF1 has already been investigated. Deletions not including the residue immediately preceding the milestone phenylalanine always preserved the inhibitory properties. Additional removal of residue 16 (yeast) or residue 21 (bovine) gave conflicting results. In some reports [23,25], such truncated IF1 peptides of *B. taurus*, *Candida utilis*, *S. cerevisiae*, and *Rattus norvegicus* were found to still inhibit ATPase activity, sometimes with a very low affinity for the enzyme [25]. In another report [24], the same deletion in *B. taurus* IF1 made the peptide apparently ineffective. The different procedures used probably account for these variations. In experiments showing an inhibitory effect, inhibition and ATPase assay were conducted in a single step [23], whereas in other experiments, the activity was assayed after diluting the inhibited sample [24]. As already discussed, the latter protocol probably led to the release of the truncated peptides and then to a general overestimation of K_I or even to an apparent loss of inhibitory power. Only direct assays as in reference 23 or as in the present work provide reliable values of binding parameters.

The K_I value of yIF1 Δ1–16 determined here (Fig. 4, Table 2) remains much lower than the K_I value of the yIF1 fragment 17–41 previously studied at the same pH [23]: 20 nM versus 4 μM. The following two explanations could be proposed for this high difference of affinities: 1) a non-negligible role of the residues 42–63 of yIF1 in its binding properties; and 2) a better affinity of the peptide for yeast F_1-ATPase, used here, than for the bovine F_1-ATPase, used in reference 23. Whatever it may be, the present work clearly demonstrates that yIF1 lacking all of the residues preceding Phe17 (Phe22 in bovine) is still inhibitory and binds to purified F_1-ATPase and membrane-bound F_0F_1-ATPase with a higher affinity than generally reported. By comparison, the dissociation constant of the inhibitory ε subunit of isolated photosynthetic F_1-ATPases is about 4 nM for thiol-reduced chloroplast ATPase [33,34] and 1 nM for cyanobacterial ATPase [35]. It is remarkable that even after elimination of its first 14 residues, the affinity of yIF1 for isolated mitochondrial F_1 subcomplex is comparable to the affinity of ε, a permanent component of the rotor, for isolated photosynthetic F_1 subcomplex.

Here, we confirmed that deletion of all the residues preceding Phe17 preserves the inhibitory property of IF1 but significantly decreases its affinity for its target. This indicates that wrapping the Nter extremity of IF1 around ATP synthase γ subunit does not directly participate in the inhibition process but stabilizes the inhibited complex. The K_I of PsaE-IF1 is intermediate between the K_I of yIF1 Δ1–15 and Δ1–16. It is not surprising that attaching a globular protein in Nter and deleting the Nter extremity result in similar loss of affinity because both modifications disrupt the interaction with γ.

4.4. Conclusions

Until now the role of the Nter part of IF1 had only been investigated by using truncated mutants in experiments in which kinetic aspects were not considered. Here, time-resolved experiments using progressively truncated peptides allowed to precise the role of the different amino acids of the Nter part of yIF1 in the successive

steps of the inhibition process. Adding a globular-like peptide in Nter also brought complementary information. The fact that PsaE-yIF1 chimeric protein binds to isolated F_1-ATPase almost at the same rate as yIF1 wT was rather unexpected. In SMP, this was still more surprising, although the steric hindrance due to PsaE may be partially compensated by a high positive charge (4.9 charges per PsaE-yIF1 molecule) favoring the peptide attraction by the membrane. The cavities between ATP synthase subunits are so narrow that, once attached to PsaE, the Nter extremity of IF1 could hardly present to the center of the enzymatic complex. Therefore, among the possible conformations of PsaE-yIF1, the only ones expected to allow binding are those with the Nter extremity folded backwards. Since yIF1 wT and PsaE-yIF1 have comparable k_{on} values, the proportion of favorable configurations is almost the same for both peptides. It is then probable that the Nter extremity (up to the 14th residue, see Table 2) folds backwards in the natural configuration for wT yIF1 binding. This suggests an outline of the different steps of IF1 binding to ATP synthase. In the above-described conformation, IF1 binds by its mid-part to a catalytic interface that is nucleotide-free [26] or that has just bound ATP [16,36]. In a second step, the Nter extremity winds around the γ subunit. This stabilizes the inhibited complex but only through the three residues preceding the conserved Phe17. At present time, such a step-by-step dissection of this binding mechanism can be achieved only using a kinetic approach.

Acknowledgements

Excellent technical help was provided by Gwénaëlle Moal-Raisin. We are indebted to Dr Bernard Lagoutte for constant and precious advices and suggestions. Thanks are due to Dr Ghada Ajlani for her fruitful help in molecular biology and to Dr Anja Krieger-Liszkay for her critical reading of the manuscript.

Appendix A. Supplementary data

Supplementary data to this article can be found online at doi:10.1016/j.bbabio.2010.10.002.

References

[1] P.D. Boyer, The ATP synthase—a splendid molecular machine, Annu. Rev. Biochem. 66 (1997) 717–749.
[2] H. Noji, R. Yasuda, M. Yoshida, K. Kinosita Jr., Direct observation of the rotation of F_1-ATPase, Nature 386 (1997) 299–302.
[3] T. Nishizaka, K. Oiwa, H. Noji, S. Kimura, E. Muneyuki, M. Yoshida, K. Kinosita Jr., Chemomechanical coupling in F_1-ATPase revealed by simultaneous observation of nucleotide kinetics and rotation, Nat. Struct. Mol. Biol. 11 (2004) 142–148.
[4] K. Adachi, K. Oiwa, T. Nishizaka, S. Furuike, H. Noji, H. Itoh, M. Yoshida, K. Kinosita Jr., Coupling of rotation and catalysis in F(1)-ATPase revealed by single-molecule imaging and manipulation, Cell 130 (2007) 309–321.
[5] M.E. Pullmann, G.C. Monroy, A naturally occurring inhibitor of mitochondrial adenosine triphosphatase, J. Biol. Chem. 238 (1963) 3762–3768.
[6] K. Schwerzmann, P.L. Pedersen, Regulation of the mitochondrial ATP synthase/ATPase complex, Arch. Biochem. Biophys. 250 (1986) 1–18.
[7] R.J. Van de Stadt, B.L. de Boer, K. Van Dam, The interaction between the mitochondrial ATPase (F1) and the ATPase inhibitor, Biochim. Biophys. Acta 292 (1973) 338–349.
[8] I. Husain, D.A. Harris, ATP synthesis and hydrolysis in submitochondrial particles subjected to an acid–base transition. Effects of the ATPase inhibitor protein, FEBS Lett. 160 (1983) 110–114.
[9] J. Power, R.L. Cross, D.A. Harris, Interaction of F_1-ATPase from ox heart mitochondria with its naturally occurring inhibitor protein. Studies using radio-iodinated inhibitor protein, Biochim. Biophys. Acta 724 (1983) 128–141.
[10] G. Klein, P.V. Vignais, Effect of the protonmotive force on ATP-linked processes and mobilization of the bound natural ATPase inhibitor in beef heart submitochondrial particles, J. Bioenerg. Biomembr. 15 (1983) 347–362.
[11] I. Husain, P.J. Jackson, D.A. Harris, Interaction between F_1-ATPase and its naturally occurring inhibitor protein. Studies using a specific anti-inhibitor antibody, Biochim. Biophys. Acta 806 (1985) 64–74.
[12] G. Lippe, M.C. Sorgato, D.A. Harris, Kinetics of the release of the mitochondrial inhibitor protein. Correlation with synthesis and hydrolysis of ATP, Biochim. Biophys. Acta 933 (1988) 1–11.
[13] G. Lippe, M.C. Sorgato, D.A. Harris, The binding and release of the inhibitor protein are governed independently by ATP and membrane potential in ox-heart submitochondrial vesicles, Biochim. Biophys. Acta 933 (1988) 12–21.
[14] R. Venard, D. Brèthes, M.-F. Giraud, J. Vaillier, J. Velours, F. Haraux, Investigation of the role and mechanism of IF1 and STF1 proteins, twin inhibitory peptides which interact with the yeast mitochondrial ATP synthase, Biochemistry 42 (2003) 7626–7636.
[15] V. Corvest, C. Sigalat, R. Venard, P. Falson, D.M. Mueller, F. Haraux, The binding mechanism of the yeast F_1-ATPase inhibitory peptide: role of catalytic intermediates and enzyme turnover, J. Biol. Chem. 280 (2005) 9927–9936.
[16] V. Corvest, C. Sigalat, F. Haraux, Insight into the bind-lock mechanism of the yeast mitochondrial ATP synthase inhibitory peptide, Biochemistry 46 (2007) 8680–8688.
[17] M. Satre, M.B. de Jerphanion, J. Huet, P.V. Vignais, ATPase inhibitor from yeast mitochondria. Purification and properties, Biochim. Biophys. Acta 387 (1975) 241–255.
[18] H. Matsubara, T. Hase, T. Hashimoto, K. Tagawa, Amino acid sequence of an intrinsic inhibitor of mitochondrial ATPase from yeast, J. Biochem. 90 (1981) 1159–1165.
[19] B. Norling, C. Tourikas, B. Hamasur, E. Glaser, Evidence for an endogenous ATPase inhibitor protein in plant mitochondria. Purification and characterization, Eur. J. Biochem. 188 (1990) 247–252.
[20] K.E. Polgreen, J. Featherstone, A.C. Willis, D.A. Harris, Primary structure and properties of the inhibitory protein of the mitochondrial ATPase (H(+)-ATP synthase) from potato, Biochim. Biophys. Acta 1229 (1995) 175–180.
[21] E. Cabezón, M.J. Runswick, A.G. Leslie, J.E. Walker, The structure of bovine IF(1), the regulatory subunit of mitochondrial F-ATPase, EMBO J. 20 (2001) 6990–6996.
[22] A.-C. Dianoux, A. Tsugita, G. Klein, P.V. Vignais, Effects of proteolytic fragmentations on the activity of the mitochondrial natural ATPase inhibitor, FEBS Lett. 140 (1982) 223–228.
[23] J.S. Stout, B.E. Partridge, D.A. Dibbern, S.M. Schuster, Peptide analogs of the beef heart mitochondrial F_1-ATPase inhibitor protein, Biochemistry 32 (1993) 7496–7502.
[24] M.J. van Raaij, G.L. Orriss, M.G. Montgomery, M.J. Runswick, I.M. Fearnley, J.M. Skehel, J.E. Walker, The ATPase inhibitor protein from bovine heart mitochondria: the minimal inhibitory sequence, Biochemistry 35 (1996) 15618–15625.
[25] M.S. Lebowitz, P.L. Pedersen, Protein inhibitor of mitochondrial ATP synthase: relationship of inhibitor structure to pH-dependent regulation, Arch. Biochem. Biophys. 330 (1996) 342–345.
[26] J.R. Gledhill, M.G. Montgomery, G.W. Leslie, J.E. Walker, How the regulatory protein, IF(1), inhibits F(1)-ATPase from bovine mitochondria, Proc. Natl Acad. Sci. USA 104 (2007) 15671–15676.
[27] N. Ichikawa, A. Karaki, M. Kawabata, S. Ushida, M. Mizushima, T. Hashimoto, The region from phenylalanine-17 to phenylalanine-28 of a yeast mitochondrial ATPase inhibitor is essential for its ATPase inhibitory activity, J. Biochem. 130 (2001) 687–693.
[28] J. Sambrook, E.F. Fritsch, T. Maniatis, in: C. Nolan (Ed.), Molecular Cloning: A Laboratory Manual, 2nd Ed, Cold Spring Harbor Laboratory, Cold Spring Harbor, NY, 1989.
[29] P. Barth, P. Savarin, B. Gilquin, B. Lagoutte, F. Ochsenbein, Solution NMR structure and backbone dynamics of the PsaE subunit of photosystem I from *Synechocystis sp*. PCC 6803, Biochemistry 41 (2002) 13902–13914.
[30] M. Galkin, R. Venard, J. Vaillier, J. Velours, F. Haraux, Functional transitions of F_0F_1-ATPase mediated by the inhibitory peptide IF1 in yeast coupled submitochondrial particles, Eur. J. Biochem. 271 (2004) 1963–1970.
[31] D. Thomas, P. Bron, T. Weimann, A. Dautant, M.-F. Giraud, P. Paumard, B. Salin, A. Cavalier, J. Velours, D. Brèthes, Supramolecular organization of the yeast F1Fo-ATP synthase, Biol. Cell 100 (2008) 591–601.
[32] M. Langner, K. Kubica, The electrostatics of lipid surfaces, Chem. Phys. Lipids 101 (1999) 3–35.
[33] P. Soteropoulos, K.-H. Süss, R.E. McCarty, Modifications of the gamma subunit of chloroplast coupling factor 1 alter interactions with the inhibitory epsilon subunit, J. Biol. Chem. 267 (1992) 10348–10354.
[34] X. He, M. Miginiac-Maslow, C. Sigalat, E. Keryer, F. Haraux, Mechanism of activation of the chloroplast ATP synthase. A kinetic study of the thiol modulation of isolated ATPase and membrane-bound ATP synthase from spinach by *Escherichia coli* thioredoxin, J. Biol. Chem. 275 (2000) 13250–13258.
[35] H. Yagi, H. Konno, T. Murakami-Fuse, A. Isu, T. Oroguchi, H. Akutsu, M. Ikeguchi, T. Hisabori, Structural and functional analysis of the intrinsic inhibitor subunit epsilon of F_1-ATPase from photosynthetic organisms, Biochem. J. 425 (2010) 85–94.
[36] E. Cabezón, M.G. Montgomery, A.G. Leslie, J.E. Walker, The structure of bovine F_1-ATPase in complex with its regulatory protein IF1, Nat. Struct. Biol. 10 (2003) 744–750.